*AKSU Annals of Sustainable Development, Volume 2 Number 1, June 2024; ISSN: (P) 3027-0499; ISSN: (E)3043-4955*

# AERO-GRAVITY DATA ANALYSIS FOR DELINEATING POSSIBLE CHANNELS OF MINERALIZATION MIGRATION THROUGH LINEAMENT - A CASE STUDY SOUTHEASTERN NIGER DELTA, NIGERIA

[1]Aniekan E. Ekpo, [1]Nsikak E. Bassey, [2]Nyakno J. George

[1]Department of Geology
Akwa Ibom State University
Mkpat Enin, Akwa Ibom Nigeria.

[2]Department of Physics
Akwa Ibom State University
Mkpat Enin, Akwa Ibom Nigeria

https://doi.org/10.60787/AASD-v2i1-35

## Abstract

*The Bouguer anomaly map of the southeastern part of the Niger Delta region of Nigeria exhibits important anomalies that are often identified by high gradients resulting from density contrasts between various anomaly sources. This reveals an important tectonic activity in the area. The northeastern part of the area is characterized by lack of water resources, except within lineaments. The sources of water within this area are enhanced secondary porosity releasable from faults, fractures and voids. Two complimentary approaches involving Euler deconvolution and tilt angle derivatives were employed in mapping out lineament over the entire study area. Results from the data analysis reveal several lineaments networks, trending in various directions of NE-SW, NW-SE, ENE-WSW, NNE-SSW and N-S. Altogether, 82 major lineaments were mapped using the 3D Euler depth solution technique and 58 from the tilt angle derivative technique. Total length of lineaments from 3D Euler deconvolution and tilt angle derivative within the study area are 225.8 km and 113.4 km respectively. These lineaments are of paramount importance with great potential impacts on hydrocarbon reservoirs and water flow in the area. Hence, these lineaments are recommended for further investigation as pathway for water and mineral resources.*

*Key words: Lineaments, Hydrocarbon, Underground water, mineralization*

## 1.0 Introduction

Lineaments are linear features on the Earth's surface that represent various geological phenomena, such as faults, fractures, and other structural elements. These features can play a crucial role in the exploration for mineral deposits, and their geological importance in relation to mineralization can be significant. Lineaments and faults often represent zones of weakness in the Earth's crust. Mineralizing fluids, carrying valuable elements, can migrate along these structures, leading to the deposition of minerals. The fractures associated with faults can create conduits for the movement of hydrothermal fluids. Hence, the need to be identified and studied them. Geophysical methods like seismic, gravity and magnetic methods have been used in locating lineaments

Geophysics being the application of the laws and principles of physics has the advantage of being able to image hidden structures and features that are inaccessible to direct observations and inspection, through measurements made on the surface of the earth either at a point, profile and or grid. Gravity survey method is a passive geophysical method that measures variations in the gravitational field of the earth at specific locations. These measurements can be made on the ground or on aerial platforms. Gravity method has been used for regional or large scale studies of geological structures, utilizing measurements of the Earth's gravitational field to delineate subsurface density variations (Biswas and Sharma, 2016).

In prospecting for oil and gas in the Niger Delta, gravity method has been used as a reconnaissance tool and its success depends on the different earth materials having different bulk densities that produced variations in the measured gravitational field. The aim of this study is to geologically interpret aero-gravity anomalies over the southeastern part of Niger Delta in order to map out the geologic structures such as lineaments in relation to mineral prospecting. The specific objectives of this study is to seek the relationship between basement lineaments and sedimentation and possible relationship between gravity lineaments and domestic water resources mostly in the Northeastern part of the study area.

## 2.0 Location and Geology of the study area

The area of investigation is located in the southeastern onshore part of the Tertiary Niger Delta Basin of Nigeria. It is part of Bayelsa, Imo, Rivers, Abia, Akwa Ibom and Cross River States of southern Nigeria. The area (**Figure 1**) lies between latitudes 4˚ 50' and 5˚ 50'N and longitudes 7˚ 00' and 9˚ 00'E. The study area covers approximately 24,650 km². The topographic map of the area is as shown in **Figure 2.**

According to Tuttle et al. (2015), the Niger Delta Basin is an extensional rift basin that is situated in the Gulf of Guinea on the passive continental margin close to Nigeria's western coast. It is thought to have access to Cameroon, Equatorial Guinea, and São Tomé and Príncipe. It is a very rich hydrocarbon province and one of the greatest Tertiary Deltas in the world (Doust, 1990; Effiong et al., 2021). According to Okiwelu et al. (2013) and Tuttle et al. (2015), it has a subaerial area of roughly 75,000 km², a total area of 300,000 km², and a sediment volume of 500,000 km³. It is estimated that nine to twelve km of sediment fill beneath the surface (Merki, 1972; Evamy et al., 1978; Fatoke, 2010; Okiwelu et al., 2013). The fact that the basin is made up of many geologic formations suggests how this basin was formed, as well as the regional and large scale tectonics of the area. The basin being an extensional basin is flanked by other basins in the area, which formed from similar processes. According to Lehner and De Ruiter (1977), the basin lies in the extreme southwestern part of a larger tectonic structure, the Benue Trough. The eastern part of the basin is bounded by the Cameroon Volcanic Line and the transform passive continental margin (Fatoke, 2010).

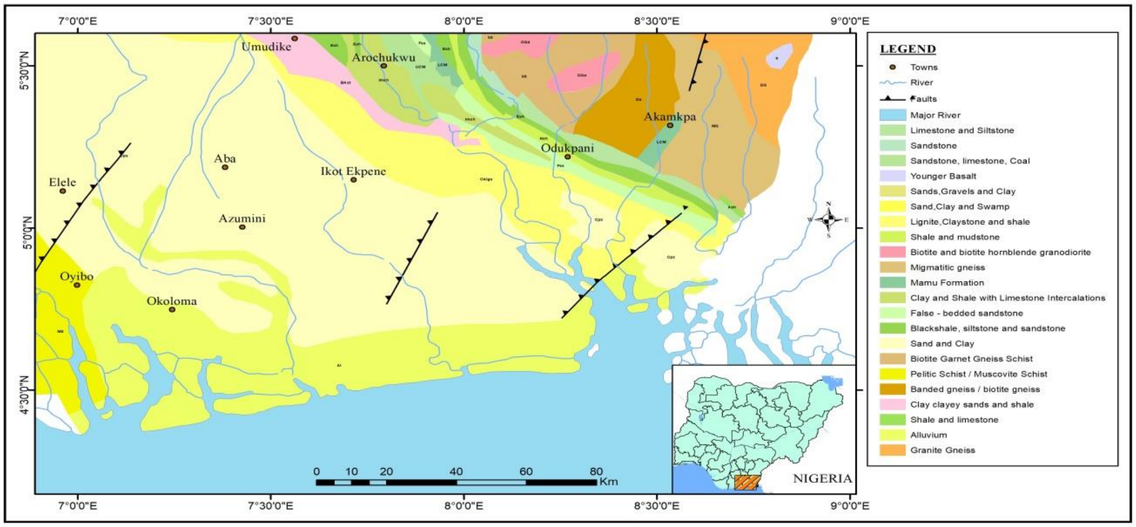

**Figure 1:** Location and Geologic map of the study area.

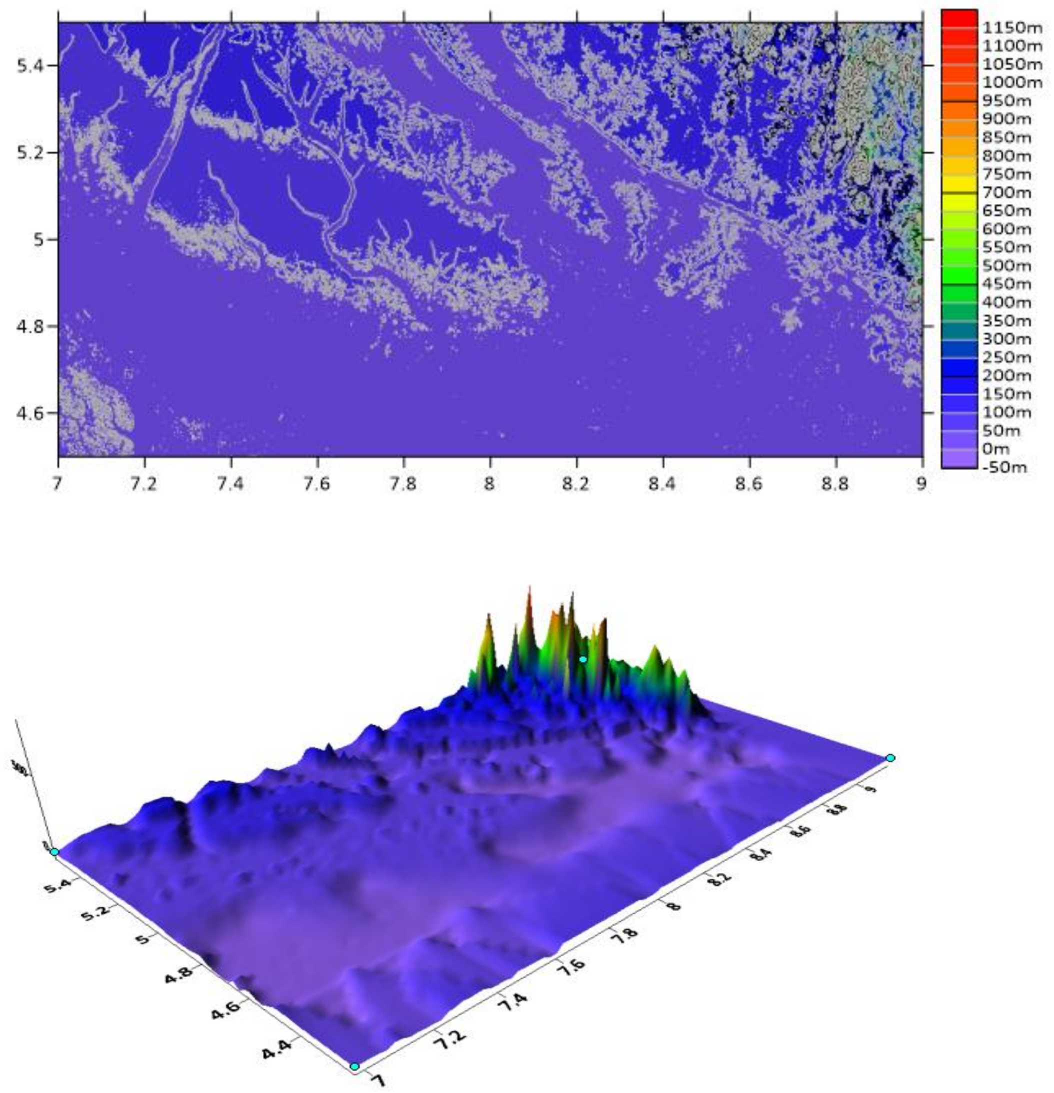

**Figure 2(a)** Topographic map of the study area. **(b)** 3D view of topographic map of the study area.

## 3.0 Methodology

The gravity field data were integrated into the World Geodetic System 84 (WGS 84) and Universal Transverse Mercator coordinate system at zone 32 of Northern hemisphere (UTM 32N) in Oasis Montaj programme (Version 7.0.1). The data directories were hosted in MAGMAP and 3D Euler deconvolution tools, which created control files that were employed in the different enhancement and modelling procedures. Euler deconvolution and Tilt Angle Derivative (TAD) maps were employed in the interpretation of gravity data.

### 3.1 Data Acquisition

The airborne gravity data used for this studies was acquired and assembled by Fugro Airborne Surveys, Canada between 2005 and 2010 for Nigerian Geological Survey Agency (NGSA). These data were acquired using the Flux- Adjusting surface data assimilation system with flight-line space of 0.1 km, tie line space of 0.5 km and terrain clearance ranging from 0.08-0.1 km along 826,000 lines. Notably, the observed potential field data exhibited significantly higher resolution compared to the 1970 aero-geophysical data, rendering them suitable for mineral and petroleum investigations, as well as geological mapping (Ekwok et al., 2020). Fugro Airborne Surveys also conducted additional requisite potential field data treatments and reductions. The raw airborne gravity data underwent processing to Bouguer data, involving the removal of instrumental drift, correction trends, Free-Air, elevation (terrain correction), Bouguer slab, and latitude, before undergoing Quality Control and Validation. The data utilized in this study were processed into Bouguer gravity gridded data, presented as color raster format imageries (see Figure 3).

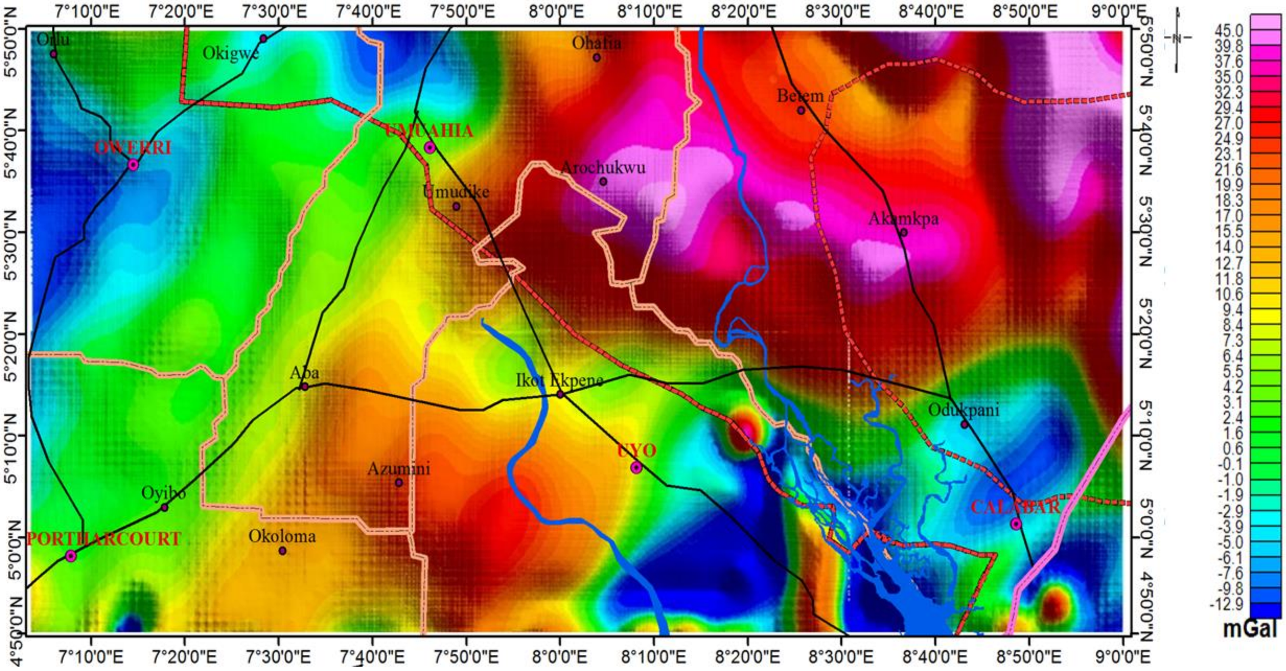

**Fig. 3:** Bouguer anomaly map of the study area.

### 3.2 Euler De-convolution

Euler de-convolution, a well-established technique in geophysics and has been employed in various forms for the analysis of gravity or magnetic data. Rooted in Euler's equation of homogeneity (Hood, 1965), this technique, originally developed for magnetic data analysis, has now been adapted for gravity data analysis and interpretation.

Thompson (1982) demonstrated the usefulness of Euler de-convolution in expediting the interpretation of potential field data, particularly in discerning geological structures and depth. This method aids in the interpretation of the gravity field by determining the location of anomalous bodies through the analysis of gravity gradients, pulse gravity fields, and constraints on body geometry (Odek et al., 2014).

The following is a review of Euler's basic de-convolution concepts and also derivation of Euler's de-convolution tensor for gravity tensor gradient. The technique applies Euler equation of homogeneity.

$$(x - x_0)Tzy + (y - y_0)Tzy + (z - z_0)Tzz = N(Bz - Tz) \qquad (1)$$

If we consider the vertical component of gravity anomaly of a body, Tz with homogeneous gravitational field, then the co-ordinates $x_0$, $y_0$ and $z_0$ are the unknown coordinates of the source body whose edges or center is being estimated and x, y, and z are the known coordinates of the gravity gradients of the observation point. The three value Tzx, Tzy, Tzz are therefore the gravity gradients $\frac{\partial T}{\partial x}, \frac{\partial T}{\partial y}$ $and$ $\frac{\partial T}{\partial z}$ measured along directions x, y and z. N is thus the structural index and Bz is the regional gravity value being estimated. Rewriting Equation (1), we get:

$$\mathrm{xTzx} + \mathrm{yTzy} + \mathrm{zTzz} + \mathrm{NTz} = x_0\mathrm{Tzx} + y_0\mathrm{Tzy} + z_0\mathrm{Tzz} + \mathrm{NBz} \qquad (2)$$

In equation (2) there are four parameters that are unknown; $x_0$, $y_{0,}z_0$and $B_z$ within a selected window of n number of data points available for solving the four unknown parameters. If N is greater than 4, these parameters can be estimated using other techniques such as Moore-Penrose inversion (Lawson and Hanson, 1974). The system uses a least squares method to solve Euler's equation simultaneously for each grid position within a window and then determines the anomaly position, depth, and base level for a specific gravity source. The obtained Euler deconvolution solution was applied to the Bouguer anomaly map with a specific structure indexes (SI) due to the acquisition parameters and window size. For the Bouguer gravity data, a structural index = 0, which indicates the presence of dyke, sill, step, and ribbon was used. Maximum depth tolerance of 3 with a window size of 10 was applied. Maximum acceptable distance of 32000 m, which is half the search window and a flying height of 100 m, was used in the analysis.

### 3.2.2 Tilt Angle Derivative (TDR)

The tilt angle derivative (TDR) is less sensitive to noise than other filtering techniques when using higher order derivatives (Akin et al., 2011). It is applied to show the borders or edge of geologic structures generating the gravity anomalies. TDR is defined as the ratio of the vertical derivative of anomalies to the horizontal derivative. Mathematically it is given as:

$$\theta = tan^{-1}\left(\frac{\left(\frac{\delta^2 A}{\delta z^2}\right)}{THD_{(x,y)}}\right) \qquad (3)$$

where total horizontal derivative, $THD_{(x,y)}$ is defined as;

$$\mathrm{TH}D_{(x,y)} = \left[\left(\frac{\delta A}{\delta x}\right)^2 + \left(\frac{\delta A}{\delta y}\right)^2\right]^{\frac{1}{2}} \qquad (4)$$

### 3.3 Lineaments Extraction

The process of extracting lineaments from these maps entailed the identification and accentuation of linear trends. The methodology employed is outlined as follows: The Euler deconvolution and Tilt Angle Derivative data were converted into raster images, facilitating the visualization of patterns and anomalies. Subsequently, thresholding techniques were applied to accentuate significant values in the maps, aiding in the identification of regions potentially featuring lineaments. Fine-tuning the thresholds played a crucial role in highlighting the desired linear features. Image processing filters were utilized to filter the maps and enhance linear features, followed by the application of skeletonization algorithms to streamline the highlighted features into one-pixel-wide lines, simplifying their representation. Connectivity analyses were conducted to scrutinize the extracted features, eliminating isolated pixels or small fragments and concentrating on continuous linear trends. The raster images were then vectorized, converting the extracted lineaments into vector formats for more accessible analysis and interpretation. Finally, the extracted lineaments were cross-referenced with the geological context of the area to ensure alignment with the geological setting.

## 4.0 Results

### 4.1 Euler deconvolution

The Euler deconvolution technique has become a valuable tool in geophysical analysis, particularly in delineating subsurface structures from potential field data. Its origins trace back to the work of Thompson in 1982, who first applied Euler deconvolution to profiled data. Subsequently, Reid et al. in 1990 extended its application to gridded data, enhancing its versatility. Euler deconvolution which serves as a method to estimate the locations and depths of linear subsurface features such as lineaments, geological contacts, faults, dikes, and sills, hinges its effectiveness upon a thorough understanding of the causative body's type and characteristics. This understanding is typically achieved by defining a structural index, as introduced by Salem et al. in 2008, which represents the rate of change of the field relative to the geometry of the source, providing crucial insights into the underlying structures. In this studies, 3D Euler deconvolution was applied to the Bouguer data, aiming to precisely detect the locations and depths of various lineaments and faults within the studyarea. Furthermore, this advanced techniques allos for the mapping of the structural extent of geological bodies, offering a comprehensive view of subsurface features and their relationships.

The Euler 3D deconvolution depth solution map (Figure 4) delineates the depth variations within the study area comprehensively. Depths range from a minimum of less than -111.4 meters to a maximum exceeding -7767.4 meters. The orientation of subsurface lineaments and fault structures exhibit diverse alignments, including NNW-SSE, NE-SW, and E-W, reflecting the predominant trends observed in the Niger Delta's lineament structure. Areas highlighted in white on the map indicate regions where structural indexes were challenging to estimate reliably due to low local wave numbers. Consequently, in these sections, the model has assigned a local wave number of zero to maintain consistency. Geologic structures, both on the surface and subsurface, manifest elliptical and elongated shapes, contributing to the overall complexity and heterogeneity of the study area's geological framework.

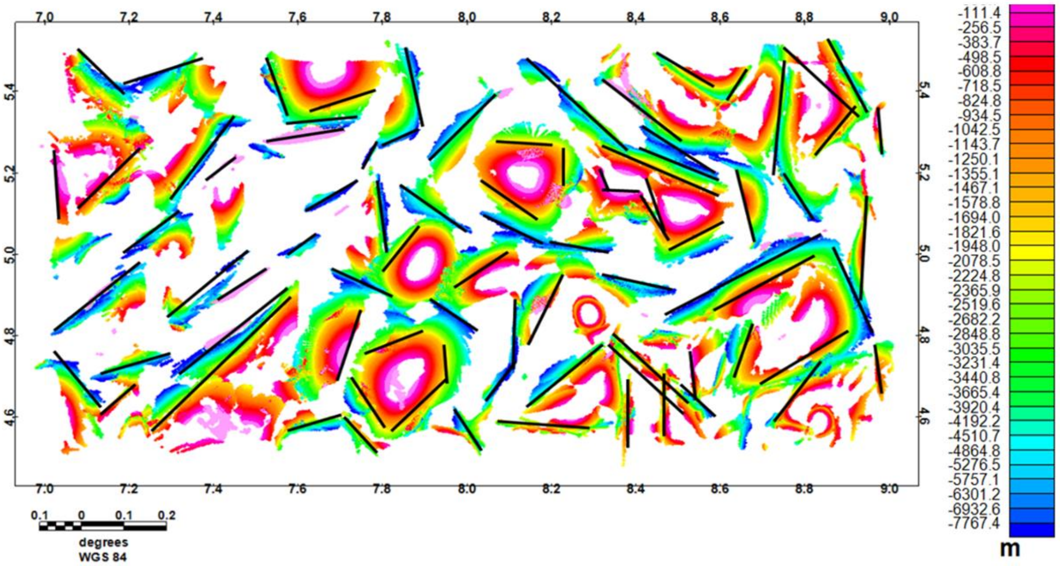

**Figure 4:** Euler 3D depth solution map showing depth distribution to causative bodies, lineaments and their structral boundries.

## 4.2 Tilt Angle Derivative (TAD)

Tilt angle derivative (**fgure 5**), which is very useful for mapping shallow basement structures and mineral exploration targets involving the mathematical operations of FFT (Fast Fourier Transform), which is the default filter and Convolution, was used to locate vertical contacts. The vertical contacts are mostly indicated by horizontal changes, which are seen mostly at geologic structural borders, faults/contacts and they are characterized by TAD values of 0 mGal on the map.

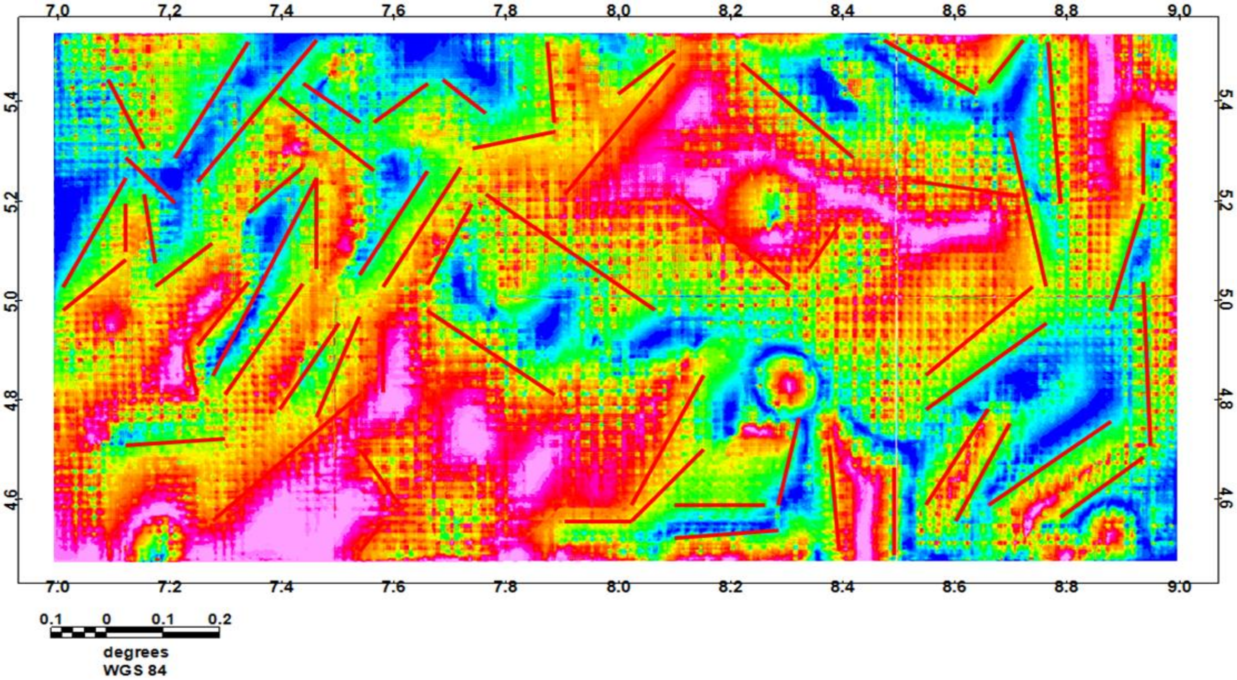

**Figure 5:** Tilt Angle Derivatives Map showing prominent lineaments boundaries

## 5.0 Discussion

### 5.1 Lineaments Map of the Studied Area

The results obtained from the analysis of gravity anomalies serve to validate and refine the configuration of brittle structures identified through geological investigations, while also shedding light on previously unrecognized features. **Figures 6a and 6b** provide visual representations of prominent boundaries delineating regions characterized by notable density contrasts, which coincide with multiple unmapped linear features. Detailed insights into each of these features are elaborated upon in **Tables 1 and 2**, which present information pertaining to the 3D Euler solution and Tilt angle derivative map, respectively. Notably, the lineaments depicted on both the Tilt angle map and the 3D Euler solution map are indicative of significant geological features influencing the study area, many of which exhibit a predominantly sub-vertical orientation. Furthermore, **Tables 3 and 4** offer a comprehensive overview of the orientations of various lineament segments delineated in the structural map of the study area (as depicted in **Figures 6a and 6b).** The principal trends discerned through analysis, as illustrated in the Rose diagram **(Figure 7)**, include orientations along the N0-10°E, N45-50°E, N85-95°E, and N120-150°E axes. Notably, there is a discernible trend whereby certain faults exhibit a propensity to trend towards the NE-SW and ENE-WSW directions with increasing depth and lateral extent. This trend correlates with the direction of subduction of the Benue Trough beneath the Pan-African Mobile Belt. Moreover, the major lineaments identified in this study, which are associated with faults, serve to characterize the inherent stability of the Sahara meta-Craton and the Congo-Craton, potentially linking to the Oubanguldes Orogen (Liégeois et al., 2013). However, it is noteworthy that several faults inferred from Bouguer anomalies within the study area demonstrate a distinct tendency to trend in a NW-SE direction with increasing depth and lateral extent, indicative of a notable shift in fault geometry.

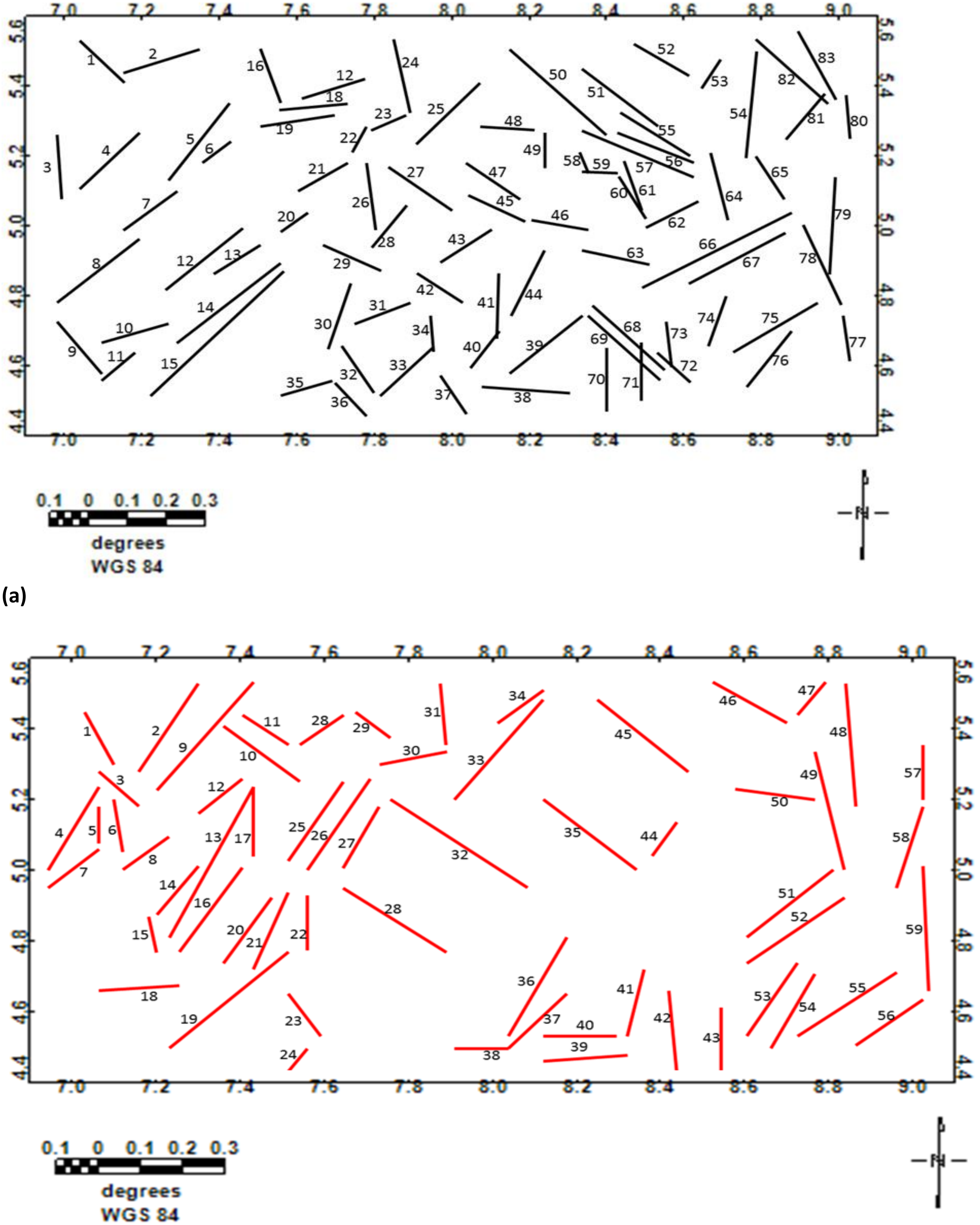

**(a)**

**(b)**

**Figure 6:** Lineament maps (**a**) extracted from 3D Euler(**b**) extracted from tilt angle

**Table 1. Orientation of different lineament segments for Euler solution map (see Figure 5a).**

| NO | Orientation (°) | Length (km) | NO | Orientation (°) | Length (km) | NO | Orientation (°) | Length (km) |
|---|---|---|---|---|---|---|---|---|
| 1 | 143 | 1.6 | 29 | 118 | 1.6 | 57 | 113 | 3.1 |
| 2 | 70 | 2.0 | 30 | 16 | 2.0 | 58 | 160 | 1.2 |
| 3 | 179 | 1.9 | 31 | 68 | 3.1 | 59 | 90 | 1.4 |
| 4 | 36 | 2.2 | 32 | 158 | 1 | 60 | 159 | 1.9 |
| 5 | 34 | 2.7 | 33 | 46 | 1.9 | 61 | 160 | 1.6 |
| 6 | 53 | 0.9 | 34 | 170 | 1 | 62 | 60 | 1.5 |
| 7 | 54 | 1.8 | 35 | 75 | 1.3 | 63 | 103 | 1.7 |
| 8 | 49 | 2.7 | 36 | 147 | 1.2 | 64 | 164 | 2.0 |
| 9 | 143 | 1.8 | 37 | 150 | 1.3 | 65 | 150 | 1.5 |
| 10 | 74 | 1.7 | 38 | 53 | 2.1 | 66 | 60 | 4.3 |
| 11 | 45 | 0.6 | 39 | 47 | 2.5 | 67 | 58 | 2.8 |
| 12 | 48 | 2.6 | 40 | 38 | 1.2 | 68 | 134 | 2.6 |
| 13 | 51 | 1.4 | 41 | 0 | 1.9 | 69 | 135 | 2.6 |
| 14 | 51 | 3.4 | 42 | 124 | 1.4 | 70 | 0 | 1.8 |
| 15 | 46 | 4.4 | 43 | 52 | 1.5 | 71 | 0 | 1.7 |
| 16 | 160 | 1.6 | 44 | 29 | 2.1 | 72 | 138 | 1.2 |
| 17 | 69 | 1.63 | 45 | 116 | 1.6 | 73 | 172 | 1.4 |
| 18 | 61 | 1.6 | 46 | 105 | 1.4 | 74 | 20 | 1.6 |
| 19 | 80 | 1.65 | 47 | 129 | 1.5 | 75 | 55 | 2.5 |
| 20 | 49 | 0.8 | 48 | 136 | 1.4 | 76 | 34 | 2.0 |
| 21 | 53 | 1.4 | 49 | 131 | 1.0 | 77 | 170 | 1.4 |
| 22 | 25 | 0.8 | 50 | 121 | 3.5 | 78 | 143 | 2.6 |
| 23 | 61 | 0.9 | 51 | 30 | 2.5 | 79 | 4 | 2.9 |
| 24 | 175 | 2.2 | 52 | 8 | 1.7 | 80 | 175 | 1.3 |
| 25 | 45 | 2.3 | 53 | 124 | 1.0 | 81 | 35 | 1.7 |
| 26 | 171 | 1.9 | 54 | 2 | 3.2 | 82 | 135 | 2.6 |
| 27 | 130 | 2.0 | 55 | 30 | 2.2 | 83 | 150 | 2.3 |
| 28 | 35 | 1.5 | 56 | 114 | 2.1 | | | |

**Table 2. Orientation of different lineament segments for tilt angle derivative map (see Figure 5b).**

| NO | Orientation (°) | Length (km) | NO | Orientation (°) | Length (km) | NO | Orientation (°) | Length (km) |
|---|---|---|---|---|---|---|---|---|
| 1 | 155 | 1.5 | 21 | 30 | 2.0 | 41 | 11 | 1.7 |
| 2 | 38 | 2.5 | 22 | 0 | 1.3 | 42 | 176 | 2.0 |
| 3 | 138 | 1.2 | 23 | 125 | 1.3 | 43 | 0 | 1.7 |
| 4 | 29 | 2.4 | 24 | 35 | 0.7 | 44 | 122 | 1.0 |
| 5 | 0 | 0.9 | 25 | 30 | 2.3 | 45 | 39 | 2.7 |
| 6 | 170 | 1.3 | 26 | 30 | 2.7 | 46 | 127 | 1.9 |
| 7 | 79 | 1.9 | 27 | 25 | 1.7 | 47 | 44 | 1.0 |
| 8 | 58 | 1.3 | 28 | 51 | 1.2 | 48 | 177 | 3.1 |
| 9 | 35 | 3.5 | 29 | 131 | 1.0 | 49 | 169 | 3.0 |
| 10 | 135 | 2.1 | 30 | 75 | 1.5 | 50 | 99 | 1.7 |
| 11 | 124 | 1.2 | 31 | 175 | 1.5 | 51 | 78 | 2.0 |
| 12 | 49 | 1.3 | 32 | 127 | 1.9 | 52 | 82 | 2.6 |
| 13 | 25 | 4.2 | 33 | 39 | 3.7 | 53 | 29 | 2.1 |
| 14 | 36 | 1.5 | 34 | 50 | 1.2 | 54 | 29 | 2.0 |
| 15 | 169 | 0.9 | 35 | 131 | 2.7 | 55 | 53 | 2.6 |
| 16 | 33 | 2.5 | 36 | 28 | 2.7 | 56 | 50 | 1.8 |
| 17 | 171 | 2.7 | 37 | 41 | 1.8 | 57 | 0 | 1.3 |
| 18 | 39 | 1.7 | 38 | 70 | 1.1 | 58 | 16 | 2.1 |
| 19 | 49 | 3.5 | 39 | 88 | 1.8 | 59 | 175 | 3.1 |
| 20 | 32 | 1.9 | 40 | 30 | 1.5 | | | |

**Table 3. Statistical analysis of Euler map for Lineament**

| Trend | Number (n) | Length (km) | Number percentage (N%) | Length percentage (L%) |
|---|---|---|---|---|
| **N-S** | 3 | 54 | 3.7 | 23.9 |
| **NNE-SSW** | 16 | 35.7 | 19.4 | 15.8 |
| **NE-SW** | 1 | 0.6 | 1.2 | 0.3 |
| **ENE-WSW** | 24 | 46.1 | 29.2 | 18.0 |
| **E-W** | 1 | 1.4 | 1.2 | 0.6 |
| **NNW-SSE** | 16 | 25.1 | 19.4 | 11.1 |
| **NW-SE** | 2 | 5.2 | 2.3 | 2.3 |
| **ESE –WNW** | 14 | 25.1 | 17.5 | 11.1 |
| **NNW-SSE** | 5 | 32.6 | 6.1 | 14.4 |
| **Total** | **82** | 225.8 | | |

**Table 4. Statistical analysis of Tilt angle derivative map for Lineament**

| Trend | Number (n) | Length (km) | Number percentage (N%) | Length percentage (L%) |
|---|---|---|---|---|
| **N-S** | 4 | 5.2 | 6.9 | 4.6 |
| **NNE-SSW** | 22 | 48.3 | 37.9 | 42.6 |
| **NE-SW** | 0 | 0 | 0 | 0 |
| **ENE-WSW** | 12 | 23.1 | 20.7 | 20.4 |
| **E-W** | 2 | 2.6 | 3.5 | 2.3 |
| **NNW-SSE** | 9 | 17.6 | 15.5 | 15.5 |
| **NW-SE** | 0 | 0 | 0 | 0 |
| **ESE -WNW** | 9 | 16.6 | 15.7 | 14.6 |
| **Total** | **58** | **113.4** | | |

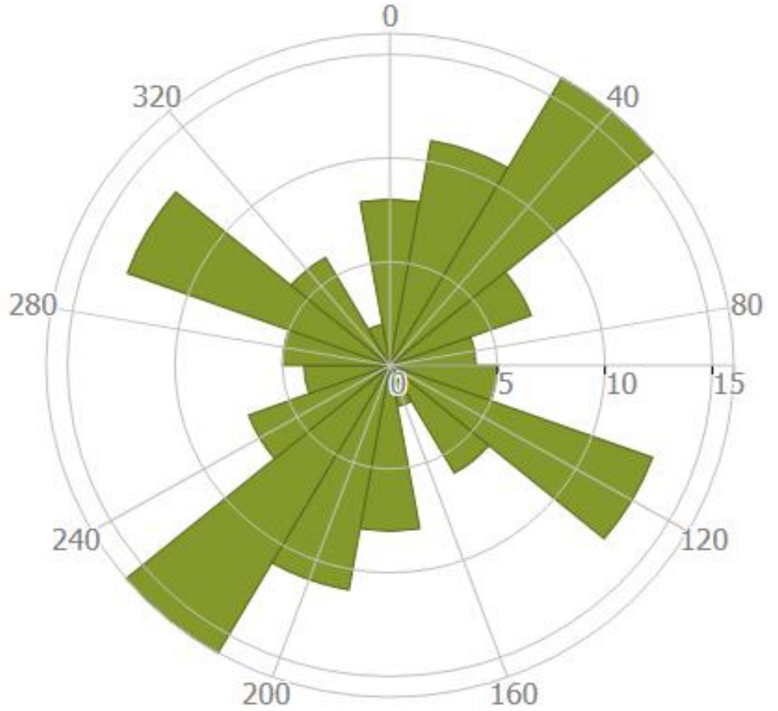

**n=82**

**(a)**

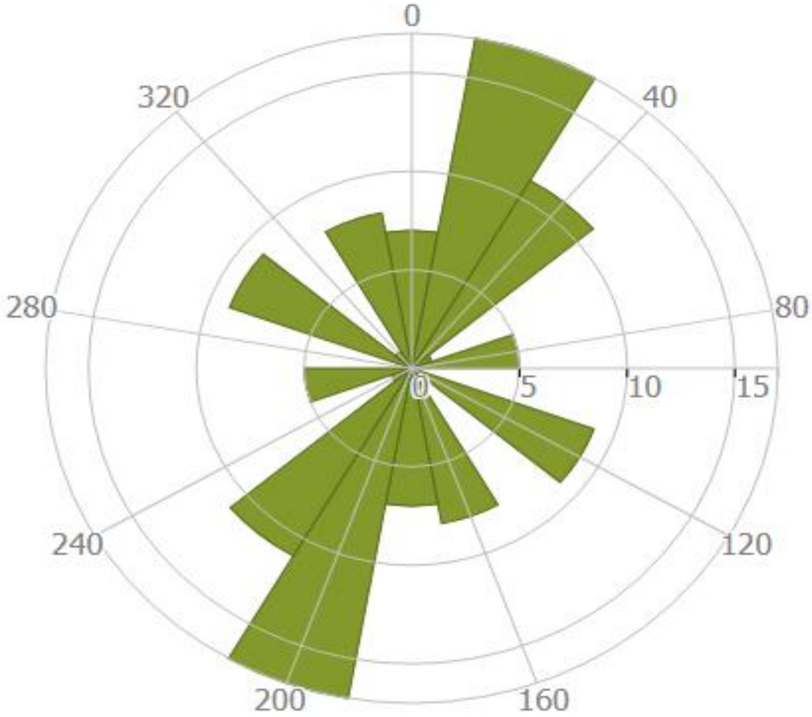

**n=58**

**(b)**

**Figure 7:** Rose diagram for **(a)** 3D Euler solution **(b)** Tilt angle derivative

The Rose diagrams show the primary directions of the lineaments in the region. The orientation of the planar and linear structures in the basement of the Southeast of Nigeria points to possible genetic relationship between the structural features (Iliya and Bassey 1993, Ekwueme 1995).

The multiple orientations of the structures indicate that the basement was subjected to poly-phase deformation, which resulted in orientation of structures in the N-S, NE-SW, E-W, ENE-WSW and NW-SE directions as indicated in the lineament maps. This corroborates the findings of Ekwueme (1995). The N-S and NE-SW trending structures are the most penetrative and are attributed to the pervasive Pan African deformation whereas the E-W, ENE-WSW and NW-SE are relicts of the Pre-Pan African deformation episodes (Grant 1978, Onyeagocha and Ekwueme 1983, Ekwueme 1994). These lineaments can be opined to be channels for flow of water and or liquid minerals. A tap into these lineaments would mean a lot to those living in the basement area, Northeast the study area, because water mostly exist in secondary porosity in that area. Also, the Southeastern part of Nigeria is endowed with a variety of solid minerals that have formed through geological processes, including precipitation. While this part of the study area is not traditionally known for extensive mineral resources, there are still notable occurrences. Precipitation-driven mineral formations often involve the deposition of minerals from solutions, usually through the evaporation of water. Here are some solid minerals in Cross River State that might have formed as a result of precipitation: Limestone can form through the precipitation of calcium carbonate from water. The Southeastern part of the study area has limestone deposits, especially around the Obubra and Yala areas that exist within lineaments. The precipitation of calcium carbonate often occurs in marine environments or from groundwater solutions. Kaolin, a clay mineral, that forms through the weathering of feldspar-rich rocks and subsequent precipitation. The Southeastern part of the study area is known for its kaolin deposits, particularly in places like Uburu and Ugep. The precipitation process involves the leaching of aluminum from feldspar and its reprecipitation and their deposition is structurally controlled by the lineaments within the area. Other minerals that exist within lineaments in the study area are Barite, Lead-Zinc, Salt (Halite) and Silica Sand.

## 6.0 Conclusion

Potential field data enhancement and analysis procedures elucidate short and long wavelength structures produced by tectonic activities in the study area. The main lineaments resulting from tectonic activities in the area were mapped, and they are believed to be the main causes of the short wavelength structures prominently observed in the Bouguer map. The 3D Euler depth solution and Tilt angle derivative maps reveal both the structural patterns of the basement as well as the depth and trend of such structures and locations of lineaments in the study area. The lineaments are believed to be channels for mineralization/migration paths for the loaded minerals in fluids through the lineament conduits. The other distinguishable features from this study are structural trends of NE-SW, NW-SE, ENE-WSW, NNE-SSW and N-S. The total length of mapped lineament observed were 225.8 km from the 3D Euler depth solution map and 113.4 km for TAD. Based on the results, geophysical gravity method is a veritable tool for reconnaissance survey and as such is recommended for structural mapping of quarrying site for earth-based company and mapping of structures in geologic basin for hydrocarbon based companies.

## FUNDING

Self-sponsored.

## DECLARATIONS

**Conflict of interest**. The author declare that they have no known competing financial interests or personal relationships that could have appeared to influence the work reported in this paper.

## HUMAN ANIMAL RIGHTS:

This article does not contain studies with human or animal subject.

## References

Akın, U. Şerifoğlu, B. &Duru, M. (2011). The use of tilt angle in gravity and magnetic methods. Bulletin of mineral research and exploration. 143. 1-12.

Biswas A, Sharma S. P (2016). Integrated geophysical studies to elicit the structure associated with Uranium mineralization around South Purulia Shear Zone, India: A Review. Ore Geology Reviews. 72:1307-1326.

Doust, H., and Omatsola, E., (1990). Niger Delta, (*in*, Edwards, J. D., and Santogrossi, P.A., eds.,) Divergent/passive Margin Basins. American Association of Petroleum Geologists Memoir 48, pp. 239-248.

Effiong, U. U., Udoyen, G.J., and Udoh, E. R. ( 2021). Ecological Determinism and Prospects of Ecotourism Development in the Niger Delta, Nigeria. AKSU Journal of Social Sciences, 1(1), 275-286.

Ekwok, S. E., Akpan, A. E. & Kudamnya, E. A., (2020). Exploratory mapping of structures controlling mineralization in Southeast Nigeria using high resolution airborne magnetic data. J*ournal of African Earth Sciences*, 162, 103700.

Ekwueme B.N, (1995) Geochemistry of crystalline basement rocks on South West Uwet, Nigeria. Dec. Ford. Journal of Pure and Applied Science. 1, pp. 15-28.

Ekwueme B.W, (1994) Basaltic Magnetism related to early stages of Benue Trough, the study dolerites of smith Eastern Nigeria. Geological Journal (29) pp. 269-276.

Evamy B. D, Harebourne J, Kamerling P, Knaap W. A, Molloy F. A, Rowlands P. H (1978). Hydocarbon habitat of Tertiary Niger Delta. Bulletin of American Association of Petroleum Geologists 62(1):1-39. Expended Abstracts, no. D04

Ezekiel J. C, Onu NN, Akaolisa C. Z, Opara A. I (2013). Preliminary Interpretation of gravity mapping over the Njaba sub-basin of Southeastern Nigeria. An implication to petroleum potential. Journal of Geology and Mining Research. 5(3):75-87.

Fatoke, OluwaseyiAdedamola (2010). Sequence stratigraphy of the Pliocene leistocene strata and shelf-margin deltas of the eastern Niger Delta, Nigeria (Ph.D.). University of Houston.

Grant, N.K. (1978). Structural distinction between a metasedimentary cover and an underlying basement in the 600m.y. old Pan African domain of Northwestern Nigeria, West Africa. Geological Society of American Bulletin, 89, 50-58.

Hood P., (1965). Gradient measurements in aeromagnetic surveying. Geophysics, Volume 30, Issue 5, Pages: 705-932ISSN (print):0016-8033ISSN (online):1942-2156

Iliya G. and Bassey N. E., (1993). Regional magnetic study of Oban and Obudu Precambrian massif, SE Nigeria. Journal of Mining and Geology. 29(2): 100-110.

Lawson, C.L., Hanson, R.J. (1974). Solving Least Squares Problems. Prentice-Hall, Englewood Cliffs.

Lehner, P. and De Ruiter, P.A.C. (1977). Structural history of Atlantic margin of Africa. *American Association of Petroleum Geologists Bulletin,*61: 961-981.

Liégeois, J. P., Abdelsalam, M., Ennih, N. and Ouabadi, A. (2013). Metacraton: Nature, genesis and behavior. Gondwana Research. 23. 220-237. 10.1016/j.gr.2012.02.016.

Merki, P. I (1972). Structural Geology of the Cenozoic Niger Delta. African Geology, University of Ibadan Press, pp. 251-260.

Murphy, B. S. (2007). Airborne Geophysics and the Indian scenario. Journal of Indian Geophysical Union, 11(1): 1-28.

Odek, A., Otieno, A. B., Ambusso, W. J. and Githiri, J. G., (2014). 2d-Euler deconvolution and forward modeling of gravity data of homa-hills geothermal prospect, kenya. Journal of Agriculture, Science and Technology, Vol. 15(1)

Okiwelu A. A, ofrey-Kulo O, Ude I. A (2013). Interpretation of regional magnetic data offshore Niger Delta reveals relationship between deep basement architecture and hydrocarbon target. Earth Science Research, 2(1):13-32.

Onyeagocha A. C. and Ekwueme B. N. (1983). Temperature-pressure distribution patterns in metamorphosed rock basement of the Nigerian Basement complex- a preliminary analysis. Journal of African Earth Science, Volume 11, Issues 1-2, pages 83-93.

Reid, A. B., Allsop, J. M., Granser, H., Millett, A. J., Somerton, I. W., (1990). Magnetic interpretation in three dimensions using Euler Deconvolution. Geophysics, vol. 55, 80–90.

Salem, A., Williams, S., Fairhead, D., Smith, R., Ravat, D., (2008). Interpretation of magnetic data using tilt angle derivatives. Geophysics vol. 73, L1–L9.

Thompson, D.T. (1982). EULDPH-A New Technique for Making Computer Estimates from Magnetic Data. Geophysics, vol. 47:31-37.

Tuttle, M., Charpentier, R., and Brownfield, M., (2015). "The Niger Delta Petroleum System: Niger Delta Province, Nigeria, Cameroon, and Equatorial Guinea, Africa". United States Geologic Survey. Retrieved 6 March 2015.

Zhang C, Mushayandebvu, M. F., Reid A. B., Fairhead J. D. and Odegard M. E. (2000). Euler De-convolution of Gravity Tensor